REPORT DOCUMENTATION PAGE

1. REPORT DATE *(DD-MM-YYYY)*	2. REPORT TYPE	3. DATES COVERED *(From - To)*
02-16-2011	Conference Proceeding	

4. TITLE AND SUBTITLE		5a. CONTRACT NUMBER
Tubercles and Localized Corrosion on Carbon Steel		
		5b. GRANT NUMBER
		5c. PROGRAM ELEMENT NUMBER
		0601153N

6. AUTHOR(S)	5d. PROJECT NUMBER
B.J. Little, R.I. Ray and J.S. Lee	
	5e. TASK NUMBER
	5f. WORK UNIT NUMBER
	73-9576-10-5

7. PERFORMING ORGANIZATION NAME(S) AND ADDRESS(ES)	8. PERFORMING ORGANIZATION REPORT NUMBER
Naval Research Laboratory Oceanography Division Stennis Space Center, MS 39529-5004	NRL/PP/7303--10-0391

9. SPONSORING/MONITORING AGENCY NAME(S) AND ADDRESS(ES)	10. SPONSOR/MONITOR'S ACRONYM(S)
Office of Naval Research 800 N. Quincy St. Arlington, VA 22217-5660	ONR
	11. SPONSOR/MONITOR'S REPORT NUMBER(S)

12. DISTRIBUTION/AVAILABILITY STATEMENT

Approved for public release, distribution is unlimited.

13. SUPPLEMENTARY NOTES

20110224055

14. ABSTRACT

The chemistry, mineralogy and microbiology of tubercles on cast iron and carbon steel were investigated. Tubercles, from diverse fresh water environments and of varying ages, consistently had an outer crust of goethite and lepidocrocite and an inner shell of magnetite. Core regions differed in structure, composition and chemistry. The presence of tubercles on carbon steel and cast iron cannot be used to conclude localized corrosion directly under the tubercles or a role for bacteria in their formation.

15. SUBJECT TERMS

tubercle, corrosion, iron-oxidizing bacteria, magnetite

16. SECURITY CLASSIFICATION OF:			17. LIMITATION OF ABSTRACT	1B. NUMBER OF PAGES	19a. NAME OF RESPONSIBLE PERSON
a. REPORT	b. ABSTRACT	c. THIS PAGE			Brenda Little
Unclassified	Unclassified	Unclassified	UL	10	19b. TELEPHONE NUMBER *(Include area code)* 228-688-5494

Tubercles and Localized Corrosion on Carbon Steel

B.J. Little, R.I. Ray and J.S. Lee Naval Research Laboratory, Stennis Space Center, MS
39529-5004, USA, blittle@nrlssc.navy.mil, Fax: 228-688-4149

T. L. Gerke
Department of Geology, University of Cincinnati, Cincinnati, OH, USA, 45221

Summary

The chemistry, mineralogy and microbiology of tubercles on cast iron and carbon steel were
investigated. Tubercles, from diverse fresh water environments and of varying ages,
consistently had an outer crust of goethite and lepidocrocite and an inner shell of magnetite.
Core regions differed in structure, composition and chemistry. The presence of tubercles on
carbon steel and cast iron cannot be used to conclude localized corrosion directly under the
tubercles or a role for bacteria in their formation.

1   Introduction

It is well established that tubercles formed on austenitic 300 series (304 or 316) stainless steel
in untreated well water (200-300 ppm [Cl⁻]) and chlorinated drinking water produce O_2
concentration cells and under-deposit corrosion. In an oxygenated environment, the area under
the tubercle, deprived of O_2, becomes a relatively small anode compared to the large
surrounding oxygenated cathode [1-4]. Metal is oxidized at the anode creating a pit and pH
decreases. The pH in the pit depends on the alloying elements. Cl⁻ migrates from the
electrolyte to the anode to neutralize charge, forming heavy metal chlorides that are extremely
corrosive. Pitting involves the conventional features of differential aeration, a large cathode:
anode surface area and the development of acidity and metallic chlorides. Under these
circumstances, the deposit or tubercle initiates the pitting and propagation is a function of
alloy and environment (e.g., Cl⁻). Tubercle formation on stainless steels is frequently
attributed to iron-oxidizing bacteria (IOB), e.g., *Gallionella* and *Leptothrix*, and the
accumulation of bound oxidized iron. In summary, tubercles cause corrosion.

In contrast, tubercle formation on cast iron and carbon steel can be the result of corrosion, i.e.,
corrosion causes tubercles [5]. Throughout this paper the term "cast iron" specifically refers to
unlined cast iron. Several authors have indicated a role for microorganisms in tubercle
formation on cast iron and carbon steels, especially IOB [6]. However, the relationships
between tubercle formation, microorganisms and corrosion of cast iron and carbon steel in
fresh water have not been established. In the following sections we present morphology,
mineralogical, chemical and microbiological data for tubercles from three sources -- Duluth-
Superior Harbor (DSH), a fresh water estuary; a drinking water distribution system (DWDS)
in the mid-western portion of the United States and a high-pressure industrial water system
(HPIW) from a US. government facility located near the Gulf of Mexico.

2   Methods and Materials

Details related to collection, embedding and imaging iron corrosion products have been reported elsewhere [7]. Operating conditions for the environmental scanning electron microscope (ESEM) and energy-dispersive spectroscopy (EDS) were described in the same publication [7]. The mineralogy of the tubercles was analyzed using a Siemens D-500 automated diffractometer system using a Cu Kα radiation at 30 mA and 40 kV. The 2θ ranged from 5° to 60°, with a 0.02° step, and a 2 second count time at each step. Crystalline phase identifications were made on the basis of peak position and peak intensities using the American Mineralogist Crystal Structure Database, the Mineral Database, and the International Center for Diffraction Data (http://rruff.geo.arizona.edu/AMS/amcsd.php, http://webmineral.com/). Approximately ten tubercles from each location were examined.

3   Results

3.1   Tubercles from untreated fresh water in DSH

The water chemistry in DSH is as follows (concentrations in mg L^{-1}): pH, 7.8-9.4; DO, 4.4-11.7 (near saturation); sulfate (SO_4^{-2}), 4-30 and chloride (Cl^-), 10.   DSH is icebound from mid-December to mid-April and during that time has a durable, well-defined ice cover. Freeze ice thicknesses in DSH range from 0.5 to 1.4 meters in addition to snow ice, stack ice, and ice from wave and splash action along harbor walls. Ice scour breaks and removes the tops of tubercles each year and tubercles reform within a few months.

DSH tubercles ranged in size from 2 x 3 cm after 1 year to 6 x 10 cm after 3 years. Tubercle height remained constant over the three-year period at about 2-5 mm. The general internal morphology of DSH tubercles consisted of a surface layer, overlying a hard shell layer that typically enclosed a core region (Figure 1). The surface layer of the DSH tubercles was made up of a reddish brown material composed of Fe(III) oxyhydroxides, primarily goethite with trace amounts of lepidocrocite. A black hard shell that had both metallic and non-metallic luster was under the surface layer and was composed predominantly of magnetite with trace amounts of goethite and lepidocrocite. The core region, yellowish-brown in color and composed of goethite and lepidocrocite, extended into the area of localized corrosion. Cores had a fibrous appearance and imaging with an ESEM demonstrated that the Fe(III) oxyhydroxides were associated with twisted bacterial stalks (Figure 2). Chromium, manganese and nickel were detected within the core regions. A feature of DSH tubercles is the well-defined stratum of copper at the base of the tubercles.
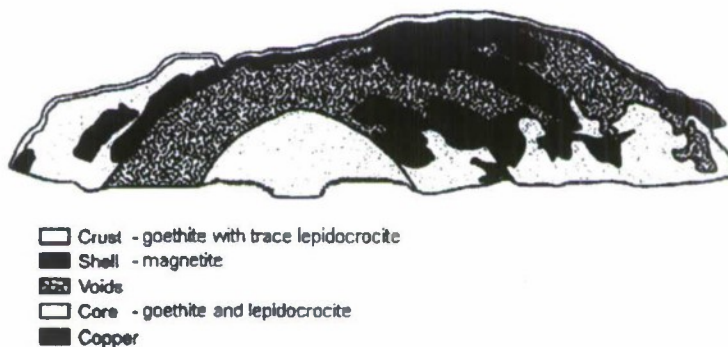

Crust - goethite with trace lepidocrocite
Shell - magnetite
Voids
Core - goethite and lepidocrocite
Copper

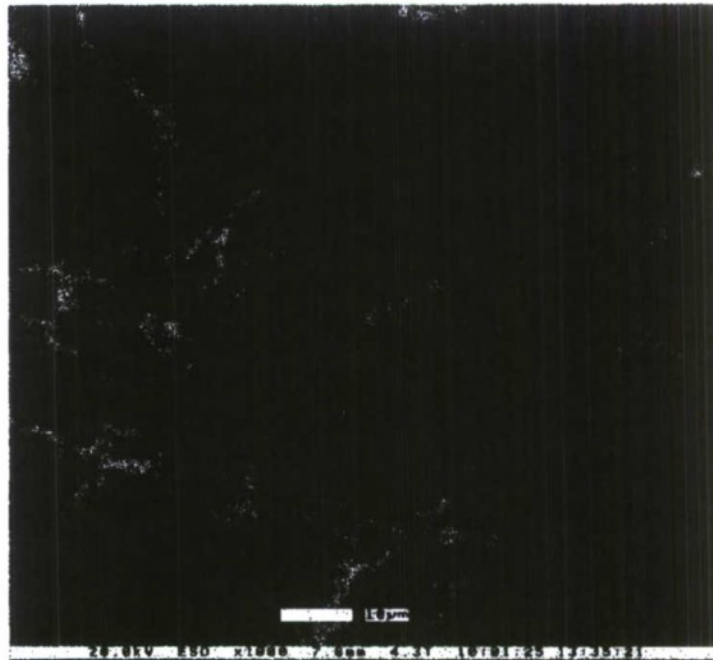*Figure 1. Diagram of DSH tubercle.*

2

Figure 2. Twisted bacterial sheaths with deposited iron within tubercle core from DSH.

All DSH tubercles were associated with localized corrosion, i.e., pitting (Figure 3). Pit volume, i.e., mass loss (depth x area) increased with time over a 3-year period. By year-3, the distribution of pit depths had increased (70-630 μm) with a metal loss of 215.25 mm^3 over 625 mm^2. Increase in pit depth with time was not linear.
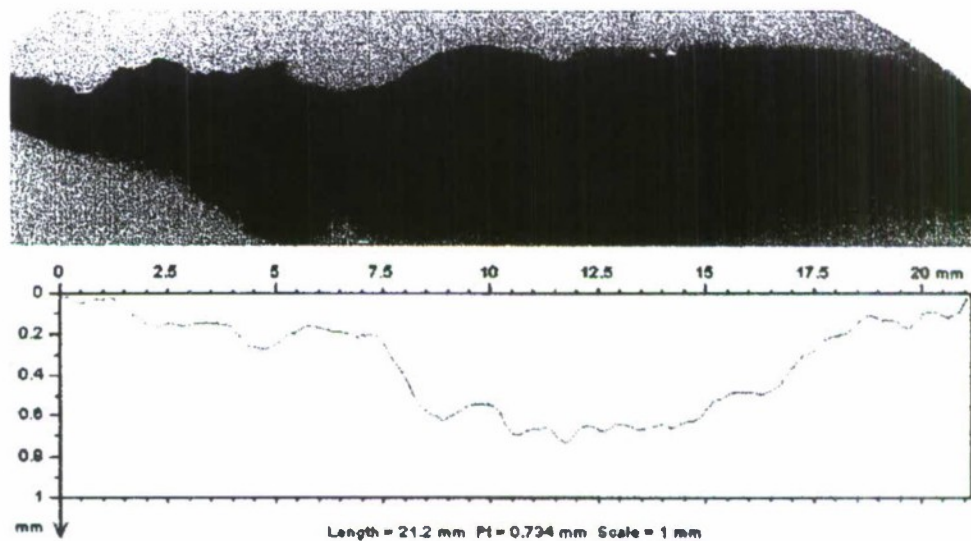

Figure 3. Cross section of tubercle and profile of pitting associated with DSH tubercle.

3

3.2 Tubercles from chlorinated DWDS

Tubercles removed from a 90 year-old cast iron pipe DWDS developed in water with the following composition (concentrations in mg L^{-1}): pH, 8.6, low to moderate hardness; alkalinity, 68; SO_4^{-2}, 98; free chlorine, 0.97 and phosphate, 0.083. The bulk water is oxygenated to saturation levels.

Tubercles from the DWDS ranged in size from a few to 10's of cm in length and in some locations had coalesced and were up to 100 cm long. An average tubercle was approximately 10 cm long and 5 cm high. The DWDS tubercles were not associated with localized corrosion (Figure 4). The general internal morphology of all tubercles examined from this DWDS consisted of a core region overlain by a hard shell and surface layer. Magnetite, lepidocrocite and goethite were the predominant iron minerals identified for the tubercles, but in different proportions.
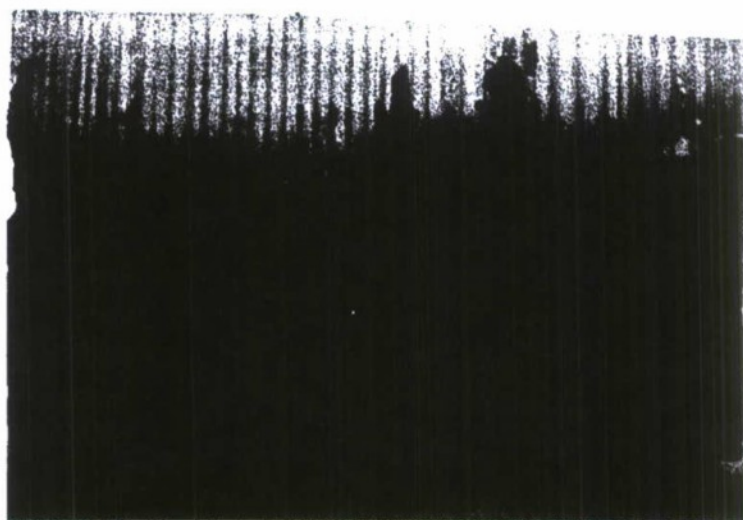

Figure 4. Cross section of tubercle and cast iron pipe from DWDS.

Based on the different proportions of the iron phases in the core, tubercles were classified into three groups: Group 1a (goethite), Group 1b (lepidocrocite), and Group 2 (magnetite) [8]. The predominant group, Group 1a, had core material that was yellowish- to reddish-brown in color and composed of goethite and trace amounts of lepidocrocite. This region was overlain by a black hard shell layer that has a metallic luster and was composed of magnetite with minor amounts of goethite and the surface layer was reddish in colored material composed primarily of goethite with minor amounts of lepidocrocite and magnetite. Magnetite veins were also present within the core regions of all tubercles in Groups 1a and 1b producing a marbled appearance and some contain subregions of filamentous textures. IOB could not be located within the core regions of tubercles from the DWDS.

Concentrations of phosphorus, calcium, lead, nickel, copper and zinc were detected by EDS throughout the core regions. Specific elements and concentrations of elements varied among tubercles from the same location and within a given region. In general the concentrations of calcium, copper, manganese, nickel, phosphorus, and zinc increased from the core to the surface layer. Aluminum concentrations were similar in the core and shell but increased in

4

the surface layer. The highest concentrations of lead were localized in the surface layer and were lowest in the shell. Significant pitting was typically not associated with these tubercles (Figure 4).

3.3   Tubercles from high-pressure industrial water (HPIW)

The HPIW system is forty-three years old and the most recent water quality indicates the following (concentrations in mg L^{-1}):   pH, 7.0, low to moderate hardness; SO_4^2, 12.2; chloride, 0.0. Tubercles were typically 5-10 cm long (developed along the axis of flow), 3-5 cm wide and 1-2 cm high. There were accumulations of lead within core regions. Tubercles from the HPIW had crusts of goethite and lepidocrocite and shells of magnetite. The core region contained biomineralized bacterial sheaths (Figure 5).   The tubercles were not associated with significant pitting.
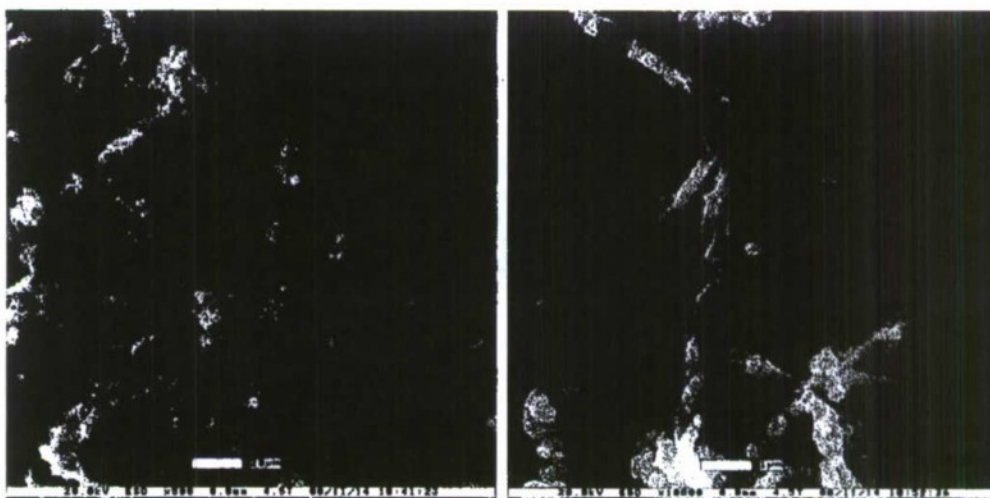

Figure 5. Twisted bacterial sheaths with deposited iron within tubercle core from HPIW.

One representative tubercle was examined in detail. Based on its internal morphology it is similar to Group 1a discussed above. It had yellowish-brown colored core material composed of goethite and moderate amounts of lepidocrocite and veinlets composed of hard black non-metallic magnetite (Figure 6). This region was overlain by a black hard shell layer that has a metallic luster and was composed of magnetite with minor amounts of goethite and lepidocrocite. A very thin (less than 0.5 mm) surface layer overlies all and was reddish in colored material. Because this layer was so thin the mineralogy and chemistry could not be examined. Biomineralized bacterial sheaths were located within the core region.

Concentrations of elements varied between the core and the hard shell layer of the representative tubercle. In general, concentrations of silica, aluminum and sodium increased from the core to the hard shell layer and there was a slight increase from the core to the hard shell layer in calcium magnesium, and lead concentrations.   The core had higher concentrations of iron and slightly higher phosphorous concentrations.
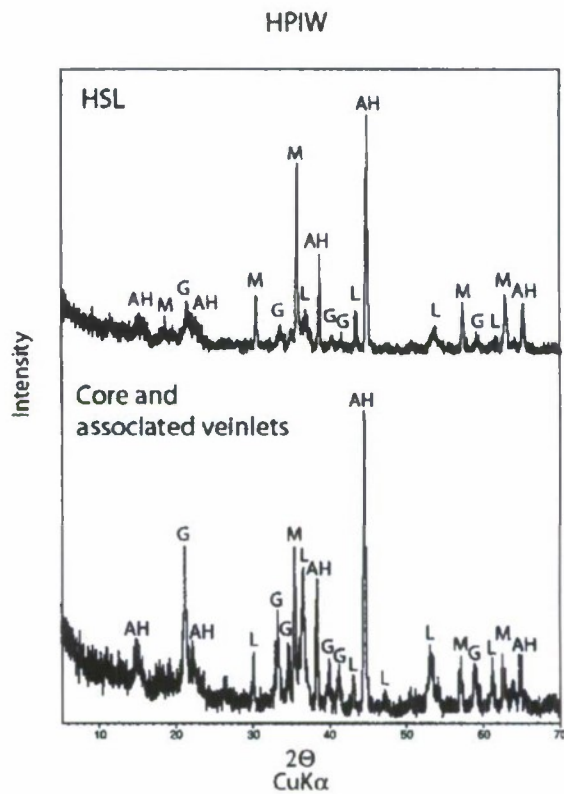
5

Figure 6. Powder X-ray diffraction patterns for the core and associated veinlets and hard shell layer (HSL) for a representative iron tubercle from HPIW. G = goethite (alpha-FeOOH), L = lepidocrocite (gamma-FeOOH), M = magnetite (Fe_3O_4), and AH = aluminum holder that the samples were analyzed.

4   Discussion

Angell [5] described abiotic and biotic mechanisms for tubercle formation on carbon steel and cast iron, i.e., mounds of corrosion products deposited above areas of "localized electrochemical corrosion" and deposition of insoluble iron by IOB. Menzies [9] described abiotic tubercle formation at breaks or discontinuities in an oxide scale exposed in an oxygenated environment. "Anodic dissolution takes place and as metal ions concentrate in the solution the solubility product of the solid hydroxide is exceeded locally and hydroxide precipitates out as a hemispherical membrane which surrounds and covers the original discontinuity. This results in effective screening of the anodic area from available oxygen and the metal at the discontinuity remains anodic." Herro [10] working with tubercles in cooling waters concluded that differential aeration cells caused tuberculation, suggesting that oxygen deficient regions below the accumulated corrosion products were anodic sites, while surrounding areas were cathodic. He indicated that tubercles grew as a result of both internal (anodic) and external (cathodic) reactions, i.e., anodic dissolution of metal resulted in the accumulation of Fe(II) (ferrous) and Fe(III) (ferric) ions and cathodic reactions outside the tubercle increased the pH and caused the precipitation of carbonate and other species whose solubility decreases with increasing pH.

6

Several investigators have demonstrated bacteria within tubercles [7, 11, 12]. Tuovinen and Hsu [13] suggested that there were zones within some tubercles that contained enough organic carbon and other nutrients to support the growth of microorganisms and microcosms with symbiotic relationships and nutrient cycling. Miller and Tiller [14] indicated, "iron bacteria, which, together with the ferric hydroxide they produce can form extensive deposits called tubercles on the inside of water pipes." Tiller [12] suggested that iron-oxidizing bacteria "encouraged" the formation of tubercles.

Several authors have described the internal morphologies of tubercles [8, 10, 15]. Herro [10] indicated that tubercles should contain the following structural features: outer crust (hematite, carbonate, silicates), inner shell (magnetite), core material (ferrous hydroxide, siderite, phosphates), fluid cavity and corroding floor. Sarin et al. [15, 16] indicated a surface layer (lepidocrocite, FeOH3, silicates, phosphates, carbonates), a shell-like layer (magnetite) and a porous core [Fe(II) and Fe(III) phases] over a corroding floor. The tubercles described in this paper, from three diverse locations, had the essential features described by previous models - core, shell and crust. The mineralogy of the crust and shell were identical to those described for tubercles isolated from other oxygen-saturated fresh water environments.

The significant difference between the Herro [10] and Sarin et al. [15, 16] model is the absence of a fluid filled cavity in the Sarin et al. [15] model. Instead Sarin et al. [15] suggested that porosity within the tubercle determined the ease with which ions migrate within the core. Their diagram indicated increased porosity at the base of the core. The cores described by Herro [10] and Gerke et al. [8] differed structurally and mineralogically. Gerke et al. [8] indicated that the majority of core material was Fe(III), either goethite or lepidocrocite, and Herro [10] described cores of Fe(II) hydroxide , siderite and phosphates. The cores from the tubercles in this study consistently contained a predominance of Fe(III) minerals, i.e., goethite and lepidocrocite.

In the present study, stalks produced by IOB and biomineralized deposits were located in tubercles from two locations – DSH and HPIW (Figures 2 and 5). Extracellular iron biomineralization has been studied extensively in fresh water [17-20]. Some iron-oxidizing microorganisms extrude polymeric structures upon which they deposit the ferric iron derived from their metabolism. Chan et al. [21] concluded that polymer directed iron hydroxide mineralization is a general phenomenon that can occur in any system containing acidic polysaccharides and iron. Banfield et al. [22] suggested that negatively charged polymers (e.g., *Gallionella* stalks) served as templates for aggregates of enzymatically produced iron oxides. Ghiorse and Ehrlich [23] suggested that microbial mineral formation can take place in intimate association with cells forming mineralized structures. They further concluded that the resulting structures could be used to identify a biological role in the formation in the absence of viable cells. Working with hyphal budding bacteria, Ghiorse and Hirsch [24] described the accumulation of positively charged iron hydroxides on negatively charged bacterial polymers. Once deposited, the iron oxides carried negative charges so that such a process could continue indefinitely without any biological activity. The only required biological input is the initial production of a negatively charged polymer. Sogaard et al. [25] described a similar process for biological iron precipitation by *Gallionella* in a polluted ground water (pH 5). Iron precipitated on the surface of the stalks until the negative charge effect was eliminated. The colloidal iron was condensed and the result was a dense deposit. Miot et al. [26] demonstrated precipitation of goethite on polymeric fibers extending from the cells of an iron-oxidizing bacterium. They also demonstrated a redox gradient, with the proportion of Fe(III) highest near the cells and the proportion of Fe(II) increasing at distance from the cell.

7

Bacteriogenic iron oxides, formed in response to chemical or bacterial oxidation of Fe(II) to Fe(III), are made up of intact and/or partly degraded remains of bacterial cells mixed with amorphous hydrous Fe(III) oxides [27]. Bacteriogenic iron oxides have reactive surfaces and act as sorbents of dissolved metal ions and enrichments of lead, cadmium, aluminum, chromium, zinc, manganese, and strontium, in addition to copper, have been reported [28, 29]. Sarin [15] reported the absorption of copper in iron corrosion scales. Gerke et al. [8] demonstrated that heavy metals, including copper, were either trapped within the structure or sorbed onto regions of the tubercles. There were differences in the heavy metals associated with the cores varied with location and within locations. In the present study, heavy metals were co-located with bacteriogenic iron oxides in two locations (DSH and HPIW). Bacterial stalks were not identified in the fibrous core of DWDS tubercles but heavy metals were concentrated in the core regions. Chromium, manganese and nickel were detected within the core regions of DSH tubercles. A feature common to all DSH tubercles was a well-defined stratum of copper at the base of the tubercles. Concentrations of phosphorus, calcium, lead, nickel, copper and zinc were detected by throughout core regions of DWDS tubercles. There were accumulations of lead within core regions of HPIW tubercles. Specific elements and concentrations of elements varied among tubercles from the same location. These differences may reflect differences in heavy metal concentrations in the fresh water in which the tubercle develops. Because of the limited water quality data available from the locations examined in this study it is impossible to relate differences in core chemistry to water chemistry.

The Herro [10] and Sarin [15, 16] models specifically describe tubercles associated with corrosion. Gerke et al. [8] described similar morphology, mineralogy and chemistry for tubercles developed in a DWDS, however, tubercles in the DWDS were not associated with localized corrosion. Angell [5] reported that the base of the tubercle was the source of "almost all of the iron that compromises the tubercle." Herro and Port [30] estimated that tubercle height was 5 to 30 times as great as the metal loss in the pit below. The Herro [10] model clearly does not describe the situation with any of the tubercles examined in this study. Tubercles formed in DSH must develop over warm summer months, are scrubbed from the surface by ice in the winter and early spring and reform. The height remained the same over a three-year period, despite the deepening pit beneath them. Tubercles in the DWDS and HPIW were not associated with localized metal loss. The cores of DSH tubercles extended into the pits and were exact replicas of the pit interior. Ray et al. [7] demonstrated that corrosion of pilings in DSH was due to a galvanic couple established between the copper layer and the iron substratum. The reducing conditions beneath the tubercles caused copper dissolved in the water to precipitate.

Data presented in this paper do not clarify the role of IOB in tubercle formation. Are IOB involved in tubercle formation or do tubercles in some environments provide conditions for IOB growth and biomineralization? Angell [5] suggested that tubercles provided anaerobic niches for sulfate reducing bacteria (SRB) and under some circumstances SRB could accelerate corrosion associated with tubercles. In an independent study, Lytle et al. [31] determined that some tubercles from the same DWDS examined in this study contained SRB.

5   Conclusions

The term "tubercle" does not describe a single morphology for corrosion products on carbon steel. The presence of tubercles on carbon steel cannot be used to conclude localized corrosion directly under the tubercles or a role for bacteria in their formation. The tubercles

8

examined in this study did have features in common – a crust of lepidocrocite and goethite and a shell of magnetite. All tubercles had a core region, but the structure and chemistry of the cores differed. Sheaths produced by iron bacteria were located in tubercles from two locations, but not the third.

6 Acknowledgements

7 References

[1] B. J. Little and J. S. Lee, *Microbiologically Influenced Corrosion*, John Wiley and Sons, Inc., Hoboken, New Jersey **2007**.

[2] S. W. Borenstein and P. B. Lindsay, *Mater. Performance* **1988**, 27, 51.

[3] G. Kobrin, *Mater. Performance* **1976**, 15, 38.

[4] D. H. Pope, R. J. Soracco and E. W. Wilde, *Mater. Performance* **1982**, 21, 43.

[5] P. Angell, *Predictive model for non-microbiologically influenced corrosion tuberculation*, EPRI, Technical Report 1003442, **2003**.

[6] R. W. Lutey, presented at *NSF-CONICET Workshop, Biocorrosion and Biofouling Proceedings*, LaPLata, Mar del Plata, Argentina, **1992**, 146.

[7] R. I. Ray, J. S. Lee and B. J. Little, *Corrosion* **2009**, 65, 707.

[8] T. L. Gerke, J. B. Maynard, M. R. Schock and D. L. Lytle, *Corros. Sci.* **2008**, 50, 2030.

[9] 1. A. Menzies, in: J. D. A. Miller (Ed.), *Microbial Aspects of Metallurgy*, American Elsevier Publishing Co., New York, NY, **1970**, 35.

[10] H. M. Herro, presented at *CORROSION / 98*, Paper 278, San Diego, CA, **1998**.

[11] T. S. Rao, T. N. Sairam, B. Viswanathan and K. V. K. Nair, *Corros. Sci.* **2000**, 42, 1417.

[12] A. K. Tiller, in: R. N. Parkins (Ed.), *Corrosion Processes*, Applied Science Publishers, London & New York, **1982**, 115.

[13] O. H. Tuovinen and J. C. Hsu, *Appl. Environ. Microbiol.* **1982**, 44, 761.

[14] J. D. A. Miller and A. K. Tiller, in: J. D. A. Miller (Ed.), *Microbial Aspects of Metallurgy*, American Elsevier Publishing Co., New York, NY, **1970**, 61.

[15] P. Sarin, V. L. Snoeyink, D. A. Lytle and W. M. Kriven, *J Environ Eng-Asce* **2004**, 130, 364.

[16] P. Sarin, V. L. Snoeyink, J. Bebee, W. M. Kriven and J. A. Clement, *Water Res.* **2001**, 35, 2961.

[17] D. Fortin, S. Langley, A. Gault, A. Ibrahim, F. G. Ferris and I. D. Clark, *Geochim. Cosmochim. Acta* **2008**, 72, A278.

[18] R. E. James and F. G. Ferris, *Chem. Geol.* **2004**, 212, 301.

[19] C. S. Chan, G. De Stasio, S. A. Welch, M. Girasole, B. H. Frazer, M. V. Nesterova, S. Fakra and J. F. Banfield, *Science* **2004**, 303, 1656.

[20] L. St.-Cyr, D. Fortin and P. G. C. Campbell, *Aquat Bot* **1993**, 46, 155.

[21] C. S. Chan, S. C. Fakra, D. C. Edwards, D. Emerson and J. F. Banfield, *Geochim. Cosmochim. Acta* **2009**, 73, 3807.

[22]   J. F. Banfield, S. A. Welch, H. Z. Zhang, T. T. Ebert and R. L. Penn, *Science* **2000**, 289, 751.

[23]   W. C. Ghiorse and H. L. Ehrlich, in: H. C. W. Skinner and R. W. Fitzpatrick (Eds.), *Iron and Manganese Biomineralization Processes in Modern and Ancient Environments*, Catena Verlag, Cremlingen, Germany, **1992**, 75.

[24]   W. C. Ghiorse and P. Hirsch, *Arch. Microbiol.* **1979**, 123, 213.

[25]   E. G. Sogaard, R. Aruna, J. Abraham-Peskir and C. B. Koch, *Appl Geochem* **2001**, 16, 1129.

[26]   J. Miot, K. Benzerara, M. Obst, A. Kappler, F. Hegler, S. Schadler, C. Bouchez, F. Guyot and G. Morin, *Appl. Environ. Microbiol.* **2009**, 75, 5586.

[27]   F. G. Ferris, *Geomicrobiol. J.* **2005**, 22, 79.

[28]   D. Dong, X. Hua, Y. Li, J. Zhang and D. Yan, *Environ. Sci. Technol.* **2003**, 37, 4106.

[29]   R. E. Martinez and F. G. Ferris, *Am. J. Sci.* **2005**, 305, 854.

[30]   H. M. Herro and R. D. Port, *NALCO Guide to Cooling Water System Failure Analysis*, McGraw-Hill International, Boston **1993**.

[31]   D. A. Lytle, T. L. Gerke and J. B. Maynard, *J Am Water Works Ass* **2005**, 97, 109.